Potential energy surface and bound states of the H 2 O–HF complex

Jérôme Loreau, Yulia Kalugina, A Faure, Ad van Der Avoird, François Lique

Potential energy surface and bound states of the H_2O-HF complex

Jérôme Loreau,[1, a)] Yulia N. Kalugina,[2] Alexandre Faure,[3] Ad van der Avoird,[4] and François Lique[5]

[1)] *KU Leuven, Department of Chemistry, B-3001 Leuven, Belgium*

[2)] *Department of Optics and Spectroscopy, Tomsk State University, 36 Lenin av., Tomsk 634050, Russia; also at Institute of Spectroscopy, Russian Academy of Sciences, Fizicheskaya St. 5, 108840 Troitsk, Moscow, Russia*

[3)] *Université Grenoble Alpes, CNRS, IPAG, F-38000 Grenoble, France*

[4)] *Institute for Molecules and Materials, Radboud University, Heyendaalseweg 135, 6525 AJ Nijmegen, The Netherlands*

[5)] *LOMC-UMR 6294, Normandie Université, Université du Havre and CNRS, 25 rue Philippe Lebon, BP 1123, 76 063 Le Havre cedex, France*

We present the first global five-dimensional potential energy surface for the H_2O–HF dimer, a prototypical hydrogen bonded complex. Large scale *ab initio* calculations were carried out using the explicitly-correlated coupled cluster approach with single- and double-excitations together with non-iterative perturbative treatment of triple excitations [CCSD(T)-F12a] with the augmented correlation-consistent aug-cc-pVTZ basis sets, in which the water and hydrogen fluoride monomers were frozen at their vibrationally averaged geometries.

The *ab initio* data points were fitted to obtain a global potential energy surface for the complex. The equilibrium geometry of the complex corresponds to the formation of a hydrogen bond with water acting as a proton acceptor and a binding energy of $D_e = 3059$ cm^{-1} (8.75 kcal/mol). The energies and wavefunctions of the lowest bound states of the complex were computed using a variational approach, and the dissociation energies of both *ortho*-H_2O-HF ($D_0 = 2089.4$ cm^{-1} or 5.97 kcal/mol) and *para*-H_2O-HF ($D_0 = 2079.6$ cm^{-1} or 5.95 kcal/mol) were obtained. The rotational constant of the complex was found to be in good agreement with the available experimental data.

[a)]Electronic mail: jerome.loreau@kuleuven.be

I. INTRODUCTION

Water is ubiquitous both on Earth and in astrophysical environments such as planetary and cometary atmospheres where it is especially abundant[1]. On earth, water plays a major role, since it is found everywhere in liquid, solid and gaseous form, and its presence seems to have been essential for the emergence of life. H_2O also has the ability to easily interact to other chemical species to form aggregates. These aggregates play a crucial role in the kinetics of the media where they are formed, in particular in the Earth's atmosphere[2], and can act as a catalyst for some chemical reactions.

The H_2O-HF heterodimer is a prototypical example of hydrogen bonded complexes, which makes it of particular importance both theoretically and experimentally. It was first observed in 1975 through infrared[3] and microwave[4] spectroscopy. The properties of this complex have been subsequently analyzed in detail experimentally in order to determine its equilibrium geometry, dipole moment[5], zero-point and equilibrium dissociation energies[6], hyperfine coupling constants[7], out-of-plane bending potential[8], and force constants for vibrational modes[9]. Additional studies of the vibrational[10–12] and rotational[13] spectrum have been reported, as well as the vibrational relaxation rates of HF by H_2O[14]. Theoretical investigations of the H_2O-HF complex have mainly focused on the determination of its equilibrium geometry and binding energy by means of various *ab initio* methods, including Hartree-Fock, second-order perturbation theory, coupled cluster, and density functional theory[15–18]. The effects of anharmonicity of the HF stretch in the complex was also explored[19]. Most recently, Sexton et al. performed a detailed study of the anharmonic corrections on the dissociation energy from second-order vibrational perturbation theory[20].

Despite the importance of the H_2O-HF complex, a global potential energy surface describing this system has never been computed. In this work, we perform large scale *ab initio* calculations by means of the explicitly correlated coupled cluster method with single, double, and perturbative triple excitations to generate a five-dimensional potential energy surface (PES). We use this PES to compute the dissociation energy, the energy of the lowest bound states of the complex, and the corresponding rotational constants.

An accurate knowledge of the interaction potential between H_2O and HF is also of interest in an astrophysical context. Hydrogen fluoride is assumed to be the dominant reservoir of fluorine in the interstellar medium[21], and it has been suggested that HF should be locked

onto icy grains in dense molecular clouds[22]. It follows from that hypothesis that HF should be present in comets formed from protostellar material. HF was indeed observed in the atmosphere of comets C/2009 P1 (Garradd)[23] and 67P/Churyumov-Gerasimenko[24], confirming that fluorine is mostly present under the form of hydrogen fluoride. In order to further improve our understanding of HF in cometary atmospheres, it is then necessary to investigate its collisional properties with the most abundant molecule, H_2O, which requires an accurate interaction potential. Indeed, non-local thermodynamic equilibrium (LTE) situations are common even in cometary atmosphere and accurate modelling of the molecular spectra requires the computation of radiative and molecular properties of astrophysical species. H_2O-molecule collisions are notoriously difficult to treat using quantum-mechanical methods, as discussed for the case of H_2O-CO in Refs.[25,26] or H_2O-HCN[27], because of the large depth and anisotropy of the potential energy surface, as well as because of the large density of molecular states of the colliding partners.

The paper is structured as follows. In Sec. II, we present the theoretical methods employed in our *ab initio* calculations, the fit of the PES, and its main features. In Sec. III we discuss the lowest bound states of the complexes *para*−H_2O-HF and *ortho*−H_2O-HF. Conclusions and perspectives are discussed in Sec. IV.

II. POTENTIAL ENERGY SURFACE

The body-fixed coordinate system employed in our calculations is presented in Fig. 1. The mutual orientation of the H_2O and HF molecules is described by one distance and a set of 4 angles (θ_1, φ_1, θ_2, φ_2). The origin of coordinates is placed at the center of mass of the H_2O molecule with the z_1-axis being the symmetry axis. The H_2O molecule lies in the x_1z_1-plane. The intermolecular vector $\mathbf{R}$ with magnitude R connects the centres of mass of H_2O and HF and the angles θ_1 and φ_1 define the position of the center of mass of HF relative to the H_2O molecule (body-fixed frame 1). On the other hand, the rotation of the HF molecule relative to the frame 2, which is parallel to the body-fixed frame 1, is defined by polar and azimuthal angles θ_2 and φ_2.

The *ab initio* calculations were performed in the rigid monomer approximation with geometrical structures corresponding to the ground vibrational state: $r_{HO} = 1.844\ a_0$, $\angle(HOH) = 104.43°$[28] and $r_{HF} = 1.749\ a_0$[29]. This is supported by geometry optimization

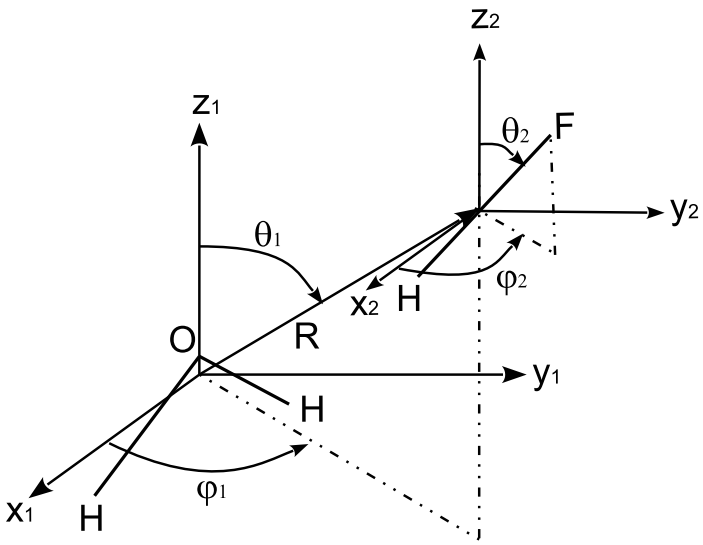

Figure 1. Coordinate system for the H_2O – HF complex.

calculations performed on the H_2O-HF dimer at the second order Møller-Plesset (MP2) and coupled cluster (CCSD(T)) levels of theory with basis sets up to quintuple-ζ which showed that the H_2O and HF monomer geometries are only weakly affected by the formation of the H_2O-HF complex[18].

The *ab initio* calculations of the potential energy surface (PES) of the electronic ground state of the H_2O-HF complex were carried out by means of the explicitly correlated coupled cluster method with single, double and perturbative triple excitations [CCSD(T)-F12a][30] with the augmented correlation-consistent triple zeta (aug-cc-pVTZ, hereafter, aVTZ) basis set[31] using MOLPRO 2010 package[32]. The optimum value for the exponent β in the correlation factor F_{12}, which is usually in the range between 1.1 a_0^{-1} and 1.5 a_0^{-1} for the AVTZ basis set[33], was set to 1.3 a_0^{-1} based on preliminary computations. The standard auxiliary basis sets and density fitting functions[34,35] (CABS(OptRI) basis sets) were used in the calculations. The five-dimensional interaction potential $V(R, \theta_1, \varphi_1, \theta_2, \varphi_2)$ was corrected for the basis set superposition error (BSSE) using the Boys and Bernardi counterpoise scheme[36]:

$$V(R, \theta_1, \varphi_1, \theta_2, \varphi_2) = E_{\mathrm{H_2O-HF}}(R, \theta_1, \varphi_1, \theta_2, \varphi_2) - E_{\mathrm{H_2O}}(R, \theta_1, \varphi_1, \theta_2, \varphi_2) - E_{\mathrm{HF}}(R, \theta_1, \varphi_1, \theta_2, \varphi_2)$$

where the energies of H_2O and HF monomers are calculated using the full basis set of the complex. The size inconsistency due to the scaling of F12 triple energy correction in

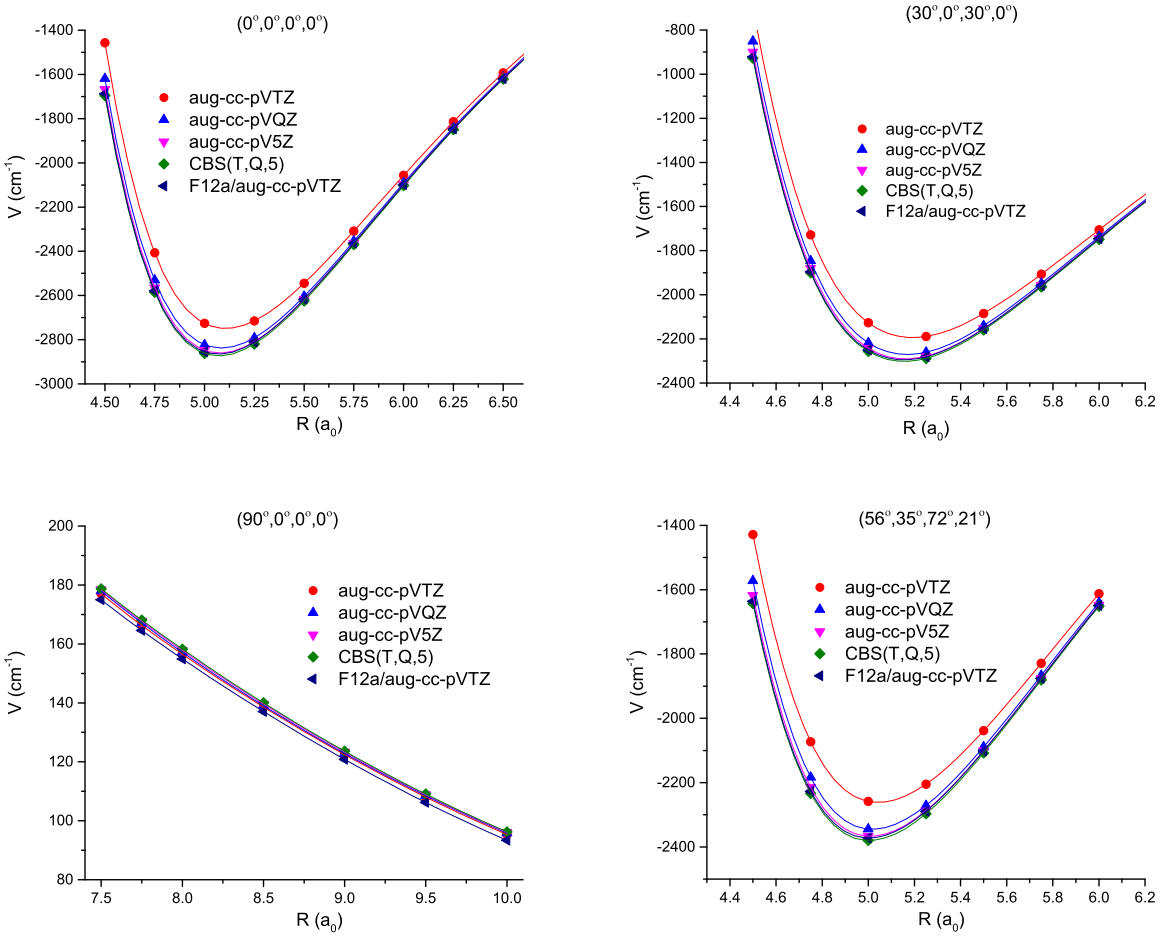

Figure 2. Radial cuts through the 5D potential energy surface for selected angular orientations $(\theta_1, \varphi_1, \theta_2, \varphi_2)$ and with various basis sets.

MOLPRO[30] was corrected by subtracting from $V(R, \theta_1, \varphi_1, \theta_2, \varphi_2)$ the asymptotic interaction energy at $R = 1000\ a_0$ which was found to be 3.35 cm^{-1} for all relative orientations.

The performance of CCSD(T)-F12a/AVTZ method is illustrated in Fig. 2, where we compare interaction energies as a function of the intermolecular distance R for four fixed angular orientations. We included results obtained using the standard CCSD(T) method with different aug-cc-pVnZ (with n=2-5) basis sets, as well as interaction energies extrapolated to the Complete Basis Set (CBS) limit using the extrapolation scheme of Peterson et al.[37]. It is seen from the figure that the results closest to the reference CCSD(T)/CBS method are obtained with the CCSD(T)-F12a approach and the aVTZ basis set, which justifies its use for the calculation of the full interaction potential.

The potential energy calculations were carried out for a large random grid of angular

orientations, i.e. for each value of intermolecular separations R the energies of about 3000 mutual orientations were calculated. 37 radial grid points were used for each angular orientation, with R varying from 3 to 30 bohr.

The analytical expansion for an asymmetric-top-linear molecule system can be written as[38]:

$$V(R,\theta_1,\varphi_1,\theta_2,\varphi_2) = \sum v_{l_1 m_1 l_2 l}(R)\bar{t}_{l_1 m_1 l_2 l}(\theta_1,\varphi_1,\theta_2,\varphi_2), \quad (1)$$

where the five body-fixed coordinates $(R,\theta_1,\varphi_1,\theta_2,\varphi_2)$ are defined in Fig. 1 and where the normalized functions $\bar{t}_{l_1 m_1 l_2 l}(\theta_1,\varphi_1,\theta_2,\varphi_2)$ are explicitly defined in Ref.[39] (see their Eqs. (5) and (6)). The indices l_1, m_1, l_2 and l refer to the tensor rank of the dependence of the interaction potential to the H_2O orientation, the HF orientation, and the collisional vector orientation, respectively. We note that a phased sum over $\pm m_1$ ensures that the angular functions are symmetric with respect to reflection in the H_2O molecule x_1z_1-plane. In the rigid-rotor approximation, the C_{2v} symmetry of H_2O also requires that m_1 is a multiple of 2. We initially included all anisotropies up to $l_1 = 9$, $l_2 = 9$, and $l = 18$, resulting in 2125 expansion functions. We then selected iteratively all significant terms using a Monte Carlo error estimator, as defined in Ref.[40], resulting in a final set of 341 expansion functions with anisotropies up to $l_1 = 9$, $l_2 = 9$, and $l = 17$. The root mean square (rms) residual, shown on Fig. 3, was found to be lower than 1 cm^{-1} for intermolecular distances larger than $R = 5.5$ bohr. The corresponding mean error[40] on the expansion functions $v_{l_1 m_1 l_2 l}(R)$ is smaller than 0.9 cm^{-1}. At shorter distances, the rms residual increases steeply due to the large anisotropy of the PES. In the region of the global minimum ($R \sim 5$ bohr, see below), however, the rms residual remains below 10 cm^{-1}, i.e. the accuracy of the fit is better than 1%. A cubic spline radial interpolation of the $v_{l_1 m_1 l_2 l}(R)$ coefficients was finally employed over the whole intermolecular distance range ($R = 3 - 30$ bohr) and it was smoothly connected to standard extrapolations (exponential and power laws at short- and long-range, respectively) using the switch function defined in Ref.[39], see their Eq. (10). The largest expansion functions are represented in Fig. 3. We note that the dipole-dipole term ($v_{1012}(R) \propto R^{-3}$) was found to strongly dominate at long-range, as expected. The whole procedure builds a `FORTRAN` routine providing the interaction potential and the (continuous) radial expansion functions suitable for bound-states as well as scattering calculations. A subroutine of the PES is provided as supplementary material.

The global minimum of the 5D PES is represented in Fig. 4. It corresponds to the

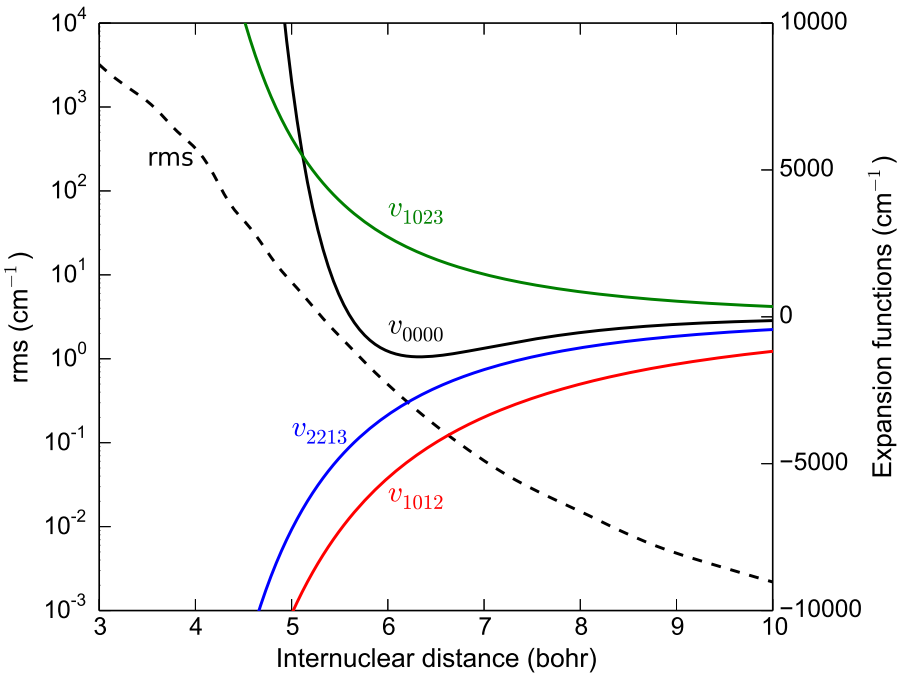

Figure 3. Plot of the rms residual of the fit, of the angular average of the H_2O-HF PES and of the largest long-range expansion functions $v_{l_1 m_1 l_2 l}(R)$ as a function of the intermolecular distance R in the range $3 - 10$ bohr. The expansion coefficients v_{1012}, v_{1023} and v_{2213} correspond to the dipole-dipole, dipole-quadrupole and quadrupole-dipole interaction terms, respectively.

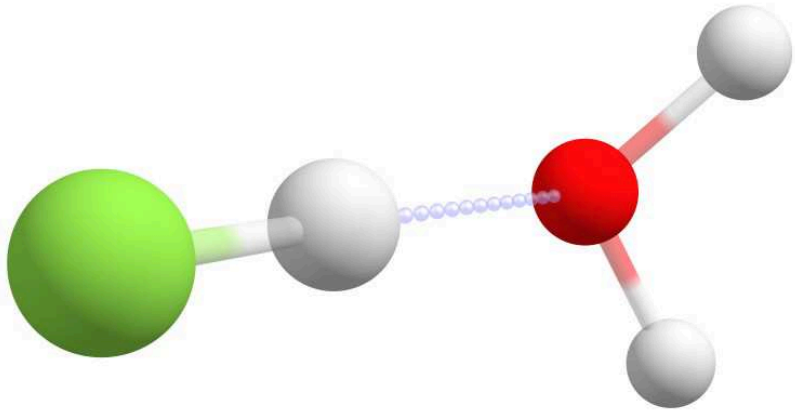

Figure 4. Configuration of the H_2O–HF complex corresponding to the global minimum.

structure with $R = 4.99\ a_0$, $\theta_1 = 51.4°$, $\varphi_1 = 90°$, $\theta_2 = 54.8°$, and $\varphi_2 = 90°$ in which a hydrogen bond is formed with the water molecule acting as proton acceptor. The close equilibrium values of θ_1 and θ_2 indicate that the HF molecule is almost along the vector **R**. The non-planar (C_s symmetry) equilibrium geometry of the complex H_2O-HF is well established, both experimentally based on an analysis of the microwave spectrum[5], and theoretically using methods such as second-order perturbation theory or coupled cluster[18,20]. The depth of the well at the global minimum as deduced from our fit is $D_e = 3059.08\ cm^{-1}$ (8.75 kcal/mol), which is in good agreement with recent calculations performed by Sexton et al.[20] with the MP2 (8.70 kcal/mol) and CCSD(T) methods with large basis sets (8.71 kcal/mol) and by Boese et al.[17] at the CCSD(T) level (8.69 kcal/mol). A value of 8.51 kcal/mol was obtained by Halkier et al.[16] by extrapolating CCSD(T) results to the basis set limit with the monomer fragments frozen at the experimental equilibrium geometry while in the present work we used the vibrationally-averaged geometries. The dissociation energy is within error bars of the value $D_e = 7.17 \pm 1.7$ kcal/mol determined by Thomas[3] based on the infrared spectrum of the complex. On the other hand, as discussed in Ref.[20], there is a large discrepancy with the experimentally determined value of $D_e = 10.25 \pm 0.2$ kcal/mol[6] derived from the intensities of rotational transitions. The experimental values of D_e were determined from the zero-point energy D_0, which will be discussed in Sec. III.

A low barrier to planarity ($\theta_1 = \theta_2 = 0$) exists. Due to the symmetry with respect to the $x_1 z_1$ plane containing H_2O, this leads to a double well potential. The height of the barrier has been estimated from experimental data to be $126 \pm 70\ cm^{-1}$[8]. In our PES the saddle point occurs for a distance $R = 5.05\ a_0$ with an energy of $-2920.9\ cm^{-1}$, corresponding to a barrier height of $138\ cm^{-1}$. This small barrier height compared to the dissociation energy indicates that the hydrogen bond in the formation of the complex H_2O-HF is only weakly directional and the planar structure can be reached easily. The potential is also attractive for the configuration in which the HF monomer acts as a hydrogen bond acceptor, but there is no associated local minimum in the potential.

Fig. 5 shows two-dimensional contour plots of our 5D PES for the H_2O–HF complex when the other coordinates are fixed to their equilibrium value. The potential is seen to be attractive for a large region of angular space. The strong anisotropy displayed by the PES (as also illustrated by Fig. 3) suggest that rotational (de-)excitation of HF in collisions with H_2O will be efficient.

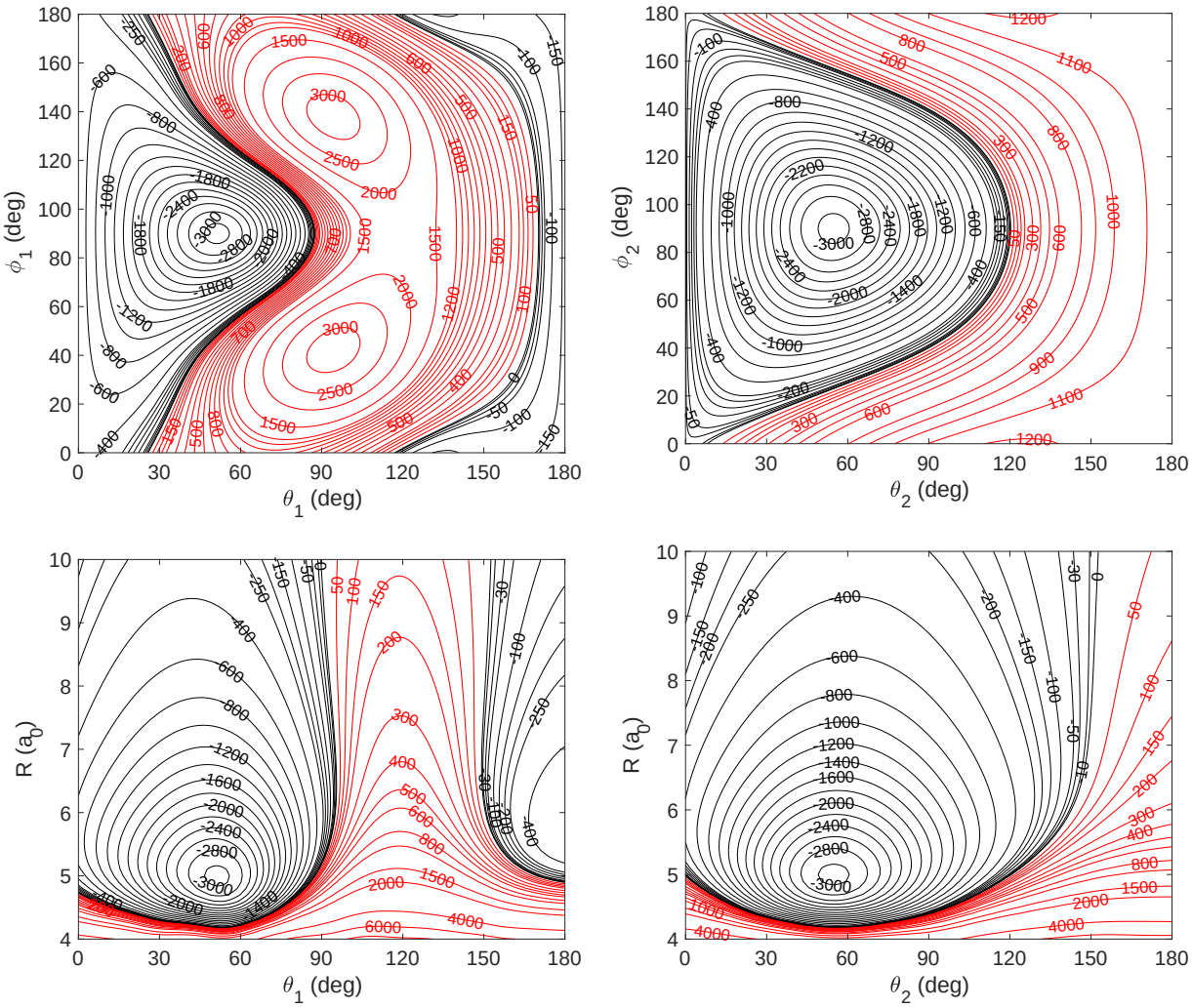

Figure 5. Cuts of the 5D PES $V(R, \theta_1, \phi_1, \theta_2, \phi_2)$. Each panel presents a two-dimensional PES while the other coordinates are fixed to the equilibrium values in the complex. Upper left panel: $R = 4.99\ a_0$, $\theta_2 = 54.8°$, $\varphi_2 = 90°$; Upper right panel: $R = 4.99\ a_0$, $\theta_1 = 51.4°$, $\varphi_1 = 90°$; Lower left panel: $\varphi_1 = 90°$, $\theta_2 = 54.8°$, $\varphi_2 = 90°$; Lower right panel: $\theta_1 = 51.4°$, $\varphi_1 = 90°$, $\varphi_2 = 90°$. The energy is in cm^{-1}.

III. BOUND STATES

The bound states calculations of the H_2O-HF complex were carried out using the variational approach that has been employed to treat other water-containing complexes such as H_2O-H_2[41], H_2O-CO[25,42] and H_2O-Ne[43,44]. The Hamiltonian of the complex is diagonalized in a basis consisting of products of angular and radial functions. The angular functions are obtained from the eigenfunctions of the two monomers. For H_2O, those are described by the

rotational quantum number j_1 and the pseudo quantum numbers k_a and k_c, corresponding respectively to the projection of j_1 along the axis of the smallest and largest moments of inertia, while for HF, we used spherical harmonics functions that are labeled by the rotational quantum number j_2. To compute the bound states, the angular basis set was truncated to $j_1 \leq 11$ and $j_2 \leq 14$. Wigner D-functions were used in the basis for the overall rotation of the complex. The radial functions are contracted discrete variable representations. We used a radial basis of 20 functions over a grid of distances of 233 points in the range $R = 3.5 - 20$ a_0. The ground vibrational state experimental values were used for the rotational constants of H_2O ($A = 27.8806$ cm^{-1}, $B = 9.2778$ cm^{-1}, $C = 14.5216$ cm^{-1}), and HF ($B = 20.5567$ cm^{-1}), along with the atomic masses of H (1.007825 u), ^{16}O (15.994915 u), and ^{19}F (18.9984 u).

The Hamiltonian for the dimer is more conveniently expressed in body-fixed (BF) coordinates, in which the z axis is along the vector $\mathbf{R}$. The new angular coordinates are denoted as $\theta(H_2O)$, the angle between the symmetry axis of H_2O and the vector $\mathbf{R}$; θ(HF), the angle between the HF axis and the vector $\mathbf{R}$; $\chi(H_2O)$, the angle of rotation of H_2O around its symmetry axis; and ϕ, the dihedral angle between the plane through $\mathbf{R}$ and the H_2O symmetry axis and the plane through $\mathbf{R}$ and the HF axis. In these coordinates, the equilibrium geometry of the complex is $\theta(H_2O) = 51.4°$, θ(HF)$= 3.4°$, $\chi(H_2O) = 90°$, and $\phi = 180°$. The small value of θ(HF) means that the HF axis is close to being parallel with the vector $\mathbf{R}$, as discussed above. The saddle point in the PES occurs for $\theta(H_2O) = \theta$(HF)$= \phi = 0°$.

The calculations make use of the molecular symmetry group G_4, the same as for H_2O, which has four irreducible representations. These correspond to distinct nuclear spin isomers: the two irreducible representations A_1^+ and A_1^- of the group have weight 1 and correspond to $para-H_2O$ (hereafter pH_2O), while the irreducible representations A_2^+ and A_2^- of the group have weight 3 and correspond to $ortho-H_2O$ (hereafter oH_2O). In addition to the total angular momentum J, the projection K of the total angular momentum on the intermolecular axis $\mathbf{R}$ can also be used to label the levels. We computed the bound states of the complex for total angular momentum values $J = 0 - 2$. Using the angular basis set described above, the energies of the levels are expected to be converged to within 0.05 cm^{-1}, while the energy differences are converged to better than 0.01 cm^{-1}.

The ground state of the pH_2O-HF complex is a Σ ($K = 0$) state with an energy of -2079.6 cm^{-1} that correlates to the $(j_1, k_a, k_c) = (0, 0, 0)$ level of H_2O. On the other hand,

the ground state of the oH$_2$O-HF complex is a Π ($K = 1$) state with an energy of -2065.6 cm^{-1}, which is higher than the ground state energy of pH$_2$O-HF by only 14.0 cm^{-1}. Since this level correlates with the ground state of the *ortho*-H$_2$O monomer, which has rotational quantum numbers $(j_1, k_a, k_c) = (1, 0, 1)$ and an energy of 23.80 cm^{-1}, the dissociation energy of oH$_2$O-HF is D_0= 2089.4 cm^{-1}, making the oH$_2$O-HF complex slightly more stable than the pH$_2$O-HF complex with D_0 = 2079.6 cm^{-1}. The difference between the dissociation energies of the *ortho* and *para* H$_2$O-HF dimers is thus only 9.8 cm^{-1}.

These dissociation energies of D_0 = 2089.4 cm^{-1} (5.97 kcal/mol) for oH$_2$O-HF or D_0 = 2079.6 cm^{-1} (5.95 kcal/mol) for pH$_2$O-HF agree well with the theoretical value of 6.01 kcal/mol obtained by Sexton et al.[20] from CCSD(T) computations with an AV5Z basis set and anharmonic effects evaluated with second-order vibrational perturbation theory. Good agreement is also found with the experimental value of $D_0 = 6.21 \pm 1.20$ kcal/mol derived by Thomas[3]. On the other hand, there is a large discrepancy with the experimental value of $D_0 = 8.20 \pm 0.07$ kcal/mol obtained by Legon et al.[6], as already discussed in Refs.[18,20]. This in turn leads to a discrepancy on the energy of the global minimum D_e (see above), since experimentally the value of D_0 was used to determine D_e. *Ab initio* methods are able to accurately describe the dissociation energies of the related dimers $(H_2O)_2$ and $(HF)_2$[20,45], which gives confidence in the calculated dissociation energies. The D_e and D_0 values obtained in the present work suggest that the zero-point energy associated with the intermolecular vibrations and internal rotations accounts for more than 30% of the binding energy.

The first excited state of pH$_2$O-HF is located about 55 cm^{-1} above the ground state and has Δ character, while a second excited state of Π character is present 90 cm^{-1} above the ground state. On the other hand, the first excited state of oH$_2$O-HF is a Σ state with an energy of 79 cm^{-1} above the ground state. In addition to the energies, for the Σ and Π states we report in Table I the value of the rotational constant B_0 obtained from the energy difference between the $J = 1$ and $J = 0$ levels (Σ states) or $J = 2$ and $J = 1$ levels (Π states) and assuming a linear structure. We find a similar value in the range $0.235 - 0.239$ cm^{-1} for all states. These values agree very well with the experimental value for the average rotational constant $B_{\rm av} = (B + C)/2$= 7202 $\pm$ 0.1 MHz[5], or 0.240 cm^{-1}, which demonstrates the accuracy of the present potential energy surface. As displayed in Table I, the Π states possess two e and f components that are almost degenerate. The splittings between the

	State	Energy (cm^{-1})	B_0 (cm^{-1})
$p$$H_2O$-HF	Σ	0	0.2362
	Δ^f	55.35	
	Δ^e	55.35	
	Π^f	90.07	0.2374
	Π^e	90.07	0.2389
$o$$H_2O$-HF	Π^e	14.00	0.2351
	Π^f	14.00	0.2371
	Σ	78.92	0.2383

Table I. Lowest bound states for $p$$H_2O$-HF and $o$$H_2O$-HF for $J = 0 - 2$. The energies are given in cm^{-1}. The origin is set at the energy to that of the lowest bound state, -2079.6 cm^{-1}.

two components are only 0.0030 cm^{-1} and 0.0039 cm^{-1} for the Π states of $p$$H_2O$-HF and $o$$H_2O$-HF, respectively. It should be noted, however, that the e and f components have different rotational constants.

A more detailed picture can be established by examining the wavefunctions corresponding to the lowest bound states reported in Table I. Fig. 6 displays four two-dimensional cuts of the wavefunction of the ground (Σ) state of $p$$H_2O$-HF. The plot of $\theta(H_2O)$ vs $\chi(H_2O)$ shows that for $\chi(H_2O)= \pm 90°$, the wavefunction has a maximum at $\theta(H_2O)= 0$ and not at the position of the global minimum of the PES, $\theta(H_2O)= 51.4°$. However, the wavefunction of the ground state is rather delocalized over the two equivalent equilibrium structures, with maximum amplitude at the saddle point of the PES. For $\chi(H_2O)= 0°$, the wavefunction peaks again at $\theta(H_2O)=0$ but it is much more localized. The plot of $\theta(H_2O)$ vs $\theta(HF)$ shows again that the wavefunction is rather delocalized, with a maximum amplitude close to the saddle point. On the other hand, the plot of $\theta(HF)$ vs ϕ demonstrates that the wavefunction is very delocalized in the torsional angle ϕ.

Fig. 7 displays plots of the ground (Π) state of $o$$H_2O$-HF, which has two components e and f. The wavefunction of the Π^f state is shown in the upper-left, upper-right, and lower-left plots. The plot of $\theta(H_2O)$ vs $\chi(H_2O)$ shows that the wavefunction has a maximum at $\chi(H_2O)= \pm 90°$ and a node at $\chi(H_2O)= 0$. As in the case of the ground state of $p$$H_2O$-HF, it is delocalized over a wide range of values of $\theta(H_2O)$ but has the largest amplitude at the

saddle point of the PES, $\theta(H_2O)$=0. Moreover, the plots of $\theta(H_2O)$ vs θ(HF), θ(HF) vs ϕ, and ϕ vs R (not shown) are very similar to those displayed in Fig. 6. The lower-right plot of Fig. 7 shows a $\theta(H_2O)$ vs $\chi(H_2O)$ contour plot of the wavefunction of the Π^e state. It presents a maximum at $\chi(H_2O)$= 0 and a node at $\chi(H_2O)$= $\pm$90°. As for the two other discussed wavefunctions, the maximum amplitude occurs at $\theta(H_2O)$= 0, but in this case the wavefunction is much more localized. We do not present other plots of the Π^e state since the wavefunction has a node at the equilibrium value $\chi(H_2O)$= 90°.

Finally, we note that Kisiel *et al.*[8] used the rotational spectrum of the complex to study the out-of-plane bending mode of the complex. They determined the energy of the first excited vibrational state of the bending mode to be 64 ± 10 cm^{-1}. In our calculations, this state corresponds to the lowest Σ state of *o*H_2O-HF, which has an energy of 64.92 cm^{-1} above the ground state of *o*H_2O-HF (or 78.92 cm^{-1} above the ground state of *p*H_2O-HF), in excellent agreement with the experimental value. A $\theta(H_2O)$ vs θ(HF) contour plot of the wave function of this state is presented in Fig. 8, illustrating the antisymmetry of wave function with respect to $\theta(H_2O)$=0 where the barrier to the out-of-plane motion is located.

IV. CONCLUSIONS

We have reported the first five-dimensional (rigid rotor) potential energy surface for the H_2O-HF complex, obtained through accurate *ab initio* calculations by means of the CCSD(T)-F12a method and an aug-cc-pVTZ basis set. The global minimum of the complex corresponds to a non-planar geometry with HF acting as a hydrogen bond donor, in good agreement with literature data. The binding energy was found to be 3059.1 cm^{-1} (8.75 kcal/mol), which is consistent with previous theoretical calculations performed using various theoretical approaches and with the experimental value of Thomas[3], but in discrepancy with the experimental value of Legon et al.[6]. The barrier to planar geometry was found to be 138 cm^{-1}. The PES has been fitted to an analytical expression, and employed in variational bound states calculations. The ground state of the complex is a Σ state for *p*H_2O-HF with a dissociation energy D_0 = 2079.6 cm^{-1} (5.95 kcal/mol), while for *o*H_2O-HF it is a Π state with D_0= 2089.4 cm^{-1} (5.97 kcal/mol). The rotational constants associated to the bound states reported in this work were also obtained, and agree well with the available microwave data. The agreement between theory and experiment on rotational transition energies gives

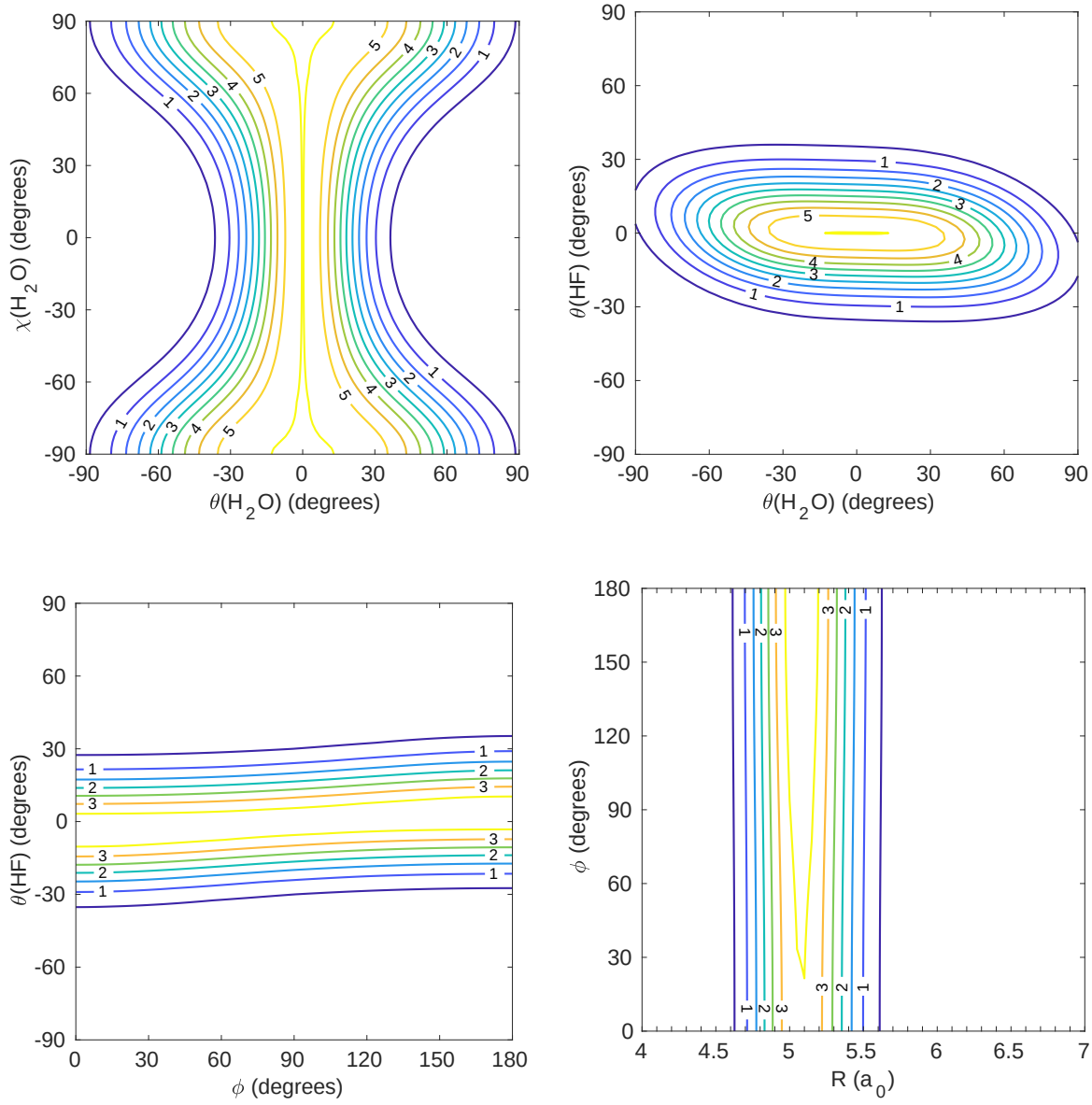

Figure 6. Wavefunction contour plots for the ground (Σ) state of pH$_2$O-HF. The coordinates not shown in the contour plots are fixed at their equilibrium values except θ(HF) which is fixed to 0° and the intermolecular distance R at 5.1 a_0, corresponding to the maximum amplitude of the wavefunctions.

confidence in the approach used in the present work. The discrepancy between the values of D_e and D_0 determined experimentally[3,6] demonstrate the need for complementary measurements on the H$_2$O-HF complex. An analysis of the wavefunctions shows that the ground state of each symmetry has a maximum amplitude at the saddle point of the PES, $\theta_1 = 0$, and not at the equilibrium value $\theta_1 = 51.4°$, with a strong dependence on the angle

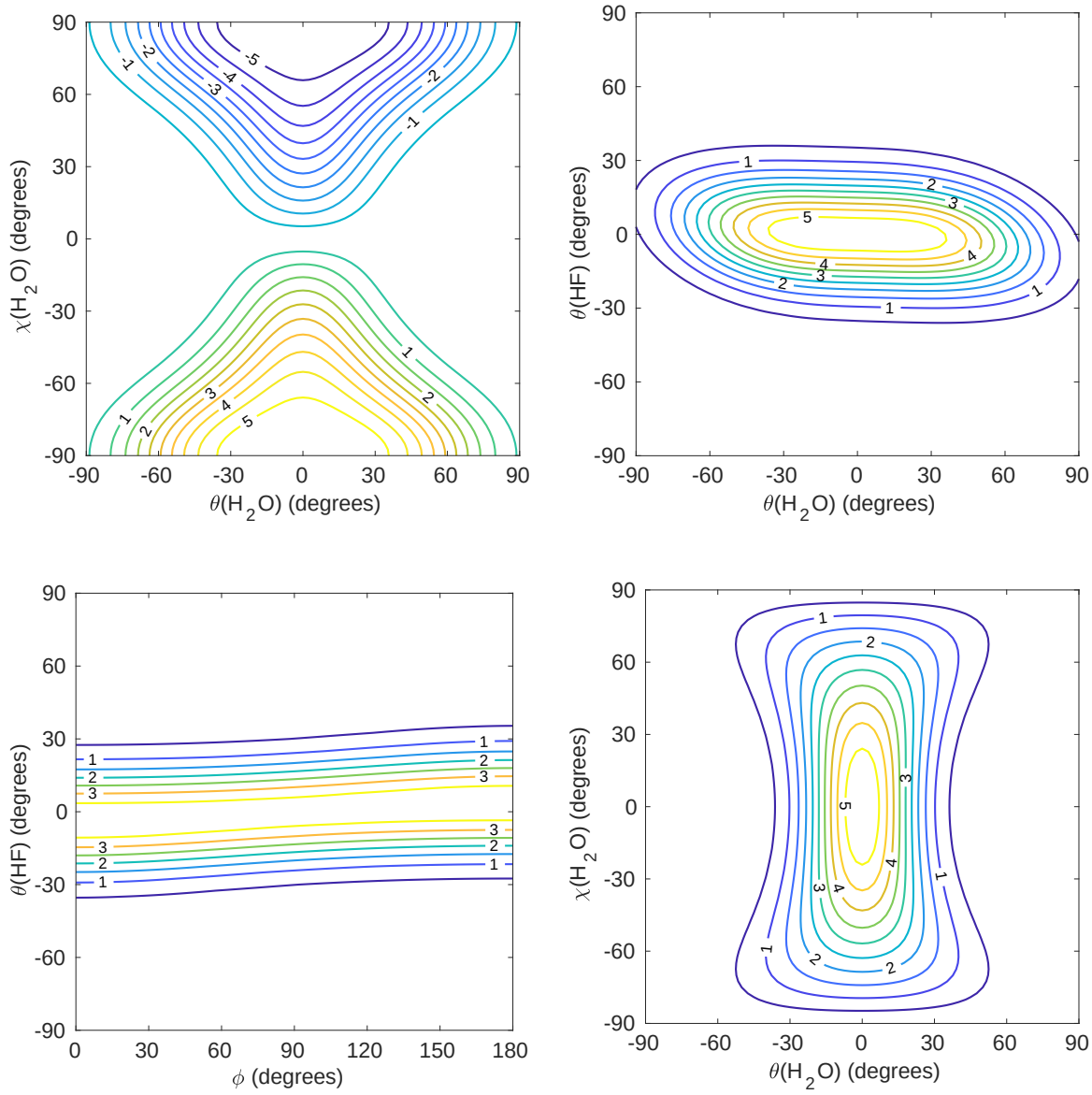

Figure 7. Wavefunction contour plots for the ground (Π) state of oH$_2$O-HF. The coordinates not shown in the contour plots are fixed at their equilibrium values except θ(HF) which is fixed to 0° and the intermolecular distance R at 5.1 a_0, corresponding to the maximum amplitude of the wavefunctions. The upper-left, upper-right, and lower-left plots are for the Π^f state, while the lower-right plot is for the Π^e state.

of rotation of H_2O around its symmetry axis.

Despite the formation of a hydrogen bond in the complex, the rigid monomer approximation is valid, as demonstrated by (i) the good agreement obtained for the position and energy of the global minimum of the PES between our and previous calculations based on

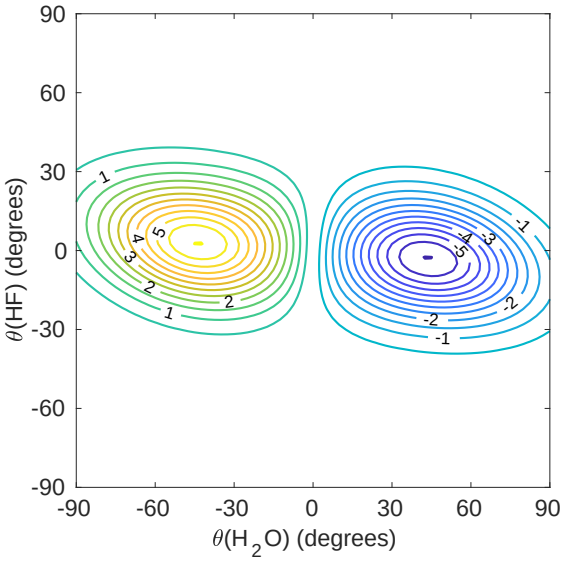

Figure 8. Wave function contour plot for the first excited state of the out-of-plane bend of the complex. The intermolecular distance R and the angle $\chi(H_2O)$ are fixed to values of 5.1 a_0 and 90°, respectively.

geometry optimization; and (ii) the good agreement with available experimental microwave data.

Since the fit of the present PES covers both the short-range and the long-range region, it can be used not only for bound states calculations but also to investigate the dynamics of H_2O-HF collisions. Such collisions are of importance in cometary atmospheres where H_2O is the most abundant molecule and HF is the main reservoir of fluorine. The study of HF in comets can also provide information about fluorine in dense molecular clouds which are progenitors of solar system analogues. Exploring the dynamics of H_2O-HF collisions will likely require the use of approximate methods similar to what has been done for H_2O-CO[46,47], as fully quantum-mechanical techniques are computationally prohibitive for such systems.

SUPPLEMENTARY MATERIAL

A `Fortran` subroutine of the potential energy surface is available as supplementary material.

ACKNOWLEDGMENTS

The resources and services used to compute the bound states were provided by the VSC (Flemish Supercomputer Center), funded by the Research Foundation - Flanders (FWO) and the Flemish Government. The results of *ab initio* calculations in Section II have been obtained under support of the RSF grant No. 17-12-01395. The angular fit of the PES was performed using the GRICAD infrastructure (https://gricad.univ-grenoble-alpes.fr), which is supported by Grenoble research communities. We acknowledge the French-Spanish collaborative project PICS (ref. PIC2017FR7). F.L. acknowledges financial support from the European Research Council (Consolidator Grant COLLEXISM, Grant Agreement 811363), the Institut Universitaire de France, and the Programme National "Physique et Chimie du Milieu Interstellaire" (PCMI) of CNRS/INSU with INC/INP cofunded by CEA and CNES.

DATA AVAILABILITY

The data that support the findings of this study are available within the article and its supplementary material.

REFERENCES

[1]E. F. van Dishoeck, E. Herbst, and D. A. Neufeld, *Chemical Reviews* **113**, 9043 (2013).

[2]I. M. Svishchev and R. J. Boyd, *J. Phys. Chem. A* **102**, 7294 (1998).

[3]R. Thomas, *Proc. R. Soc. London, Ser. A* **344**, 579 (1975).

[4]J. W. Bevan, A. C. Legon, D. J. Millen, and S. C. Rogers, *J. Chem. Soc. Chem. Commun.* , 341 (1975).

[5]J. W. Bevan, Z. Kisiel, A. C. Legon, D. J. Millen, and S. C. Rogers, *Proc. R. Soc. London A* **372**, 441 (1980).

[6]A. Legon, D. Millen, and H. M. North, *Chem. Phys. Lett.* **135**, 303 (1987).

[7]A. Legon and L. Willoughby, *Chem. Phys. Lett.* **92**, 333 (1982).

[8]Z. Kisiel, A. C. Legon, and D. J. Millen, *Proc. R. Soc. London, Ser. A* **381**, 419 (1982).

[9]Z. Kisiel, A. Legon, and D. Millen, *J. Mol. Struct.* **112**, 1 (1984).

[10]Z. Kisiel, A. Legon, and D. Millen, *J. Mol. Struct.* **131**, 201 (1985).

[11]V. P. Bulychev, E. I. Gromova, and K. G. Tokhadze, *Optics and Spectroscopy* **96**, 774 (2004).

[12]V. P. Bulychev, I. M. Grigoriev, E. I. Gromova, and K. G. Tokhadze, *Phys. Chem. Chem. Phys.* **7**, 2266 (2005).

[13]S. Belov, V. Demkin, N. Zobov, et al., *J. Mol. Spectrosc.* **241**, 124 (2007).

[14]J. K. Hancock and W. H. Green, *J. Chem. Phys.* **57**, 4515 (1972).

[15]P. A. Kollman and L. C. Allen, *J. Chem. Phys.* **52**, 5085 (1970).

[16]A. Halkier, W. Klopper, T. Helgaker, P. Jørgensen, and P. R. Taylor, *J. Chem. Phys.* **111**, 9157 (1999).

[17]A. D. Boese, J. M. L. Martin, and W. Klopper, *J. Phys. Chem. A* **111**, 11122 (2007).

[18]J. Demaison and J. Liévin, *Mol. Phys.* **106**, 1249 (2008).

[19]B. Silvi, R. Wieczorek, Z. Latajka, et al., *J. Chem. Phys.* **111**, 6671 (1999).

[20]T. M. Sexton, J. C. Howard, and G. S. Tschumper, *J. Phys. Chem. A* **122**, 4902 (2018).

[21]D. A. Neufeld and M. G. Wolfire, *Ap. J.* **706**, 1594 (2009).

[22]M. Emprechtinger, R. R. Monje, F. F. S. van der Tak, et al., *Ap. J.* **756**, 136 (2012).

[23]Bockelée-Morvan, D., Biver, N., Crovisier, J., et al., *A&A* **562**, A5 (2014).

[24]F. Dhooghe, J. De Keyser, K. Altwegg, et al., *Mon. Not. R. Astron. Soc.* **472**, 1336 (2017).

[25]Y. N. Kalugina, A. Faure, A. van der Avoird, K. Walker, and F. Lique, *Phys. Chem. Chem. Phys.* **20**, 5469 (2018).

[26]J. Loreau, A. Faure, and F. Lique, *J. Chem. Phys.* **148**, 244308 (2018).

[27]M. Dubernet and E. Quintas-Sánchez, *Molecular Astrophysics* **16**, 100046 (2019).

[28]G. Czako, E. Matyus, and A. G. Csaszar, *J. Phys. Chem. A* **113**, 11665 (2009).

[29]A. A. Mason and A. H. Nielsen, *J. Opt. Soc. Am.* **57**, 1464 (1967).

[30]H.-J. W. G. Knizia, T. B. Adler, *J. Chem. Phys.* **130**, 054104 (2009).

[31]T. H. Dunning, *J. Chem. Phys.* **90**, 1007 (1989).

[32]H.-J. Werner, P. J. Knowles, G. Knizia, et al., MOLPRO, version 2010.1, a package of ab initio programs, 2010.

[33]T. B. Adler, G. Knizia, and H.-J. Werner, *The Journal of Chemical Physics* **127**, 221106 (2007).

[34]W. Klopper, *Mol. Phys.* **99**, 481 (2001).

[35]F. Weigend, A. Köhn, and C. Hättig, *J. Chem. Phys.* **116**, 3175 (2002).

[36]S. F. Boys and F. Bernardi, *Mol. Phys.* **19**, 553 (1970).

[37]K. A. Peterson, D. E. Woon, and T. H. Dunning, Jr., *J. Chem. Phys.* **100**, 7410 (1994).

[38]T. Phillips, S. Maluendes, A. McLean, and S. Green, *J. Chem. Phys.* **101**, 5824 (1994).

[39]P. Valiron, M. Wernli, A. Faure, et al., *J. Chem. Phys.* **129**, 134306 (2008).

[40]C. Rist and A. Faure, *Journal of Mathematical Chemistry* **50**, 588 (2012).

[41]A. van der Avoird and D. Nesbitt, *J. Chem. Phys.* **134**, 044314 (2011).

[42]A. J. Barclay, A. van der Avoird, A. R. W. McKellar, and N. Moazzen-Ahmadi, *Phys. Chem. Chem. Phys.* **21**, 14911 (2019).

[43]M. P. Ziemkiewicz, C. Pluetzer, M. Wojcik, et al., *J. Chem. Phys.* **146**, 104204 (2017).

[44]M. P. Ziemkiewicz, C. Pluetzer, J. Loreau, A. van der Avoird, and D. J. Nesbitt, *J. Chem. Phys.* **147**, 214304 (2017).

[45]J. C. Howard, J. L. Gray, A. J. Hardwick, L. T. Nguyen, and G. S. Tschumper, *Journal of Chemical Theory and Computation* **10**, 5426 (2014).

[46]J. Loreau, F. Lique, and A. Faure, *Ap. J. Lett.* **853**, L5 (2018).

[47]A. Faure, F. Lique, and J. Loreau, *Mon. Not. R. Astron. Soc.* **493**, 776 (2020).